Water Vapor Uptake in Photolithographic Polymers Observed by Infrared Near-Field Scanning Optical Microscopy in a Controlled Environment

Laurie A. McDonough,[†] Bogdan Dragnea,[‡] Jan Preusser, and Stephen R. Leone*,[†]

JILA, National Institute of Standards and Technology and University of Colorado and Department of Chemistry and Biochemistry, and Department of Physics, University of Colorado, Boulder, Colorado 80309-0440

William D. Hinsberg

IBM Almaden Research Center, 650 Harry Road, San Jose, California 95120-6099

Received: November 26, 2002

An infrared near-field scanning optical microscope (NSOM) is used in a controlled environment chamber to detect water vapor uptake in thin polymer films. A chemically amplified photoresist sample composed of alternating 2 μm lines of the original 1000 nm thick poly-(*tert*-butylmethacrylate) (PTBMA) and the photochemically modified 500 nm thick poly(methacrylic acid) (PMAA) is studied both in low and high water vapor environments. The degree of water vapor absorption by the sample is measured using the infrared transmission of 2.85 μm light on a small spatial scale (<500 nm). The accompanying topographic swelling of the samples is measured using a shear-force feedback loop. Distortion of the topographic structure and variation in transmission contrast indicate that the PMAA zones absorb more water than the PTBMA regions in the water vapor environment. The PMAA swells 280 nm more than PTBMA when exposed to a partial pressure of water vapor of 2.1 kPa (16 Torr), whereas the infrared optical contrast is increased to a 6 ± 1% difference in the PMAA regions compared to the PTBMA.

Transmission near-field scanning optical microscopy (NSOM) uses a sub-wavelength aperture probe that is scanned in close proximity to the surface of a sample to overcome the diffraction limit on spatial resolution. Infrared-NSOM (IR-NSOM) provides the possibility of vibrational spectroscopy and band specificity with this high spatial resolution. Although visible light is more frequently used with NSOM, IR-NSOM has been used to study systems from semiconductors to polymers to human cells.[1−11] This work further develops the IR-NSOM by integrating it into a controlled environment chamber so that samples can be explored in controlled vapor environments. Previous work with a visible NSOM in a vacuum explored the effect of varying temperatures on semiconductor samples.[12,13] Now, additionally, samples can be exposed to various gases, and the changes they undergo can be monitored.[14]

Here we study how polymer samples react when exposed to water vapor. This topic has importance for many polymer industries, including packaging, chemical sensors, drug delivery, artificial organs, and electronics. It is particularly important in patterned chemically amplified photoresists, which are used in the fabrication of micro and nanocircuits in the electronics industry.[15,16] Many polymers swell and change shape when they absorb enough water vapor. The degree of vapor uptake and swelling depends on factors such as film processing and quality, polymer composition and density, molecular orientation of polymer chains, size and density of pores, and film thickness.[17−21] Because photochemically modified areas have a different affinity for water than the unexposed areas, swelling of the polymer can cause distortions of patterns. This can lead to problems with reproducibility and transfer of the desired mask for subsequent etching.

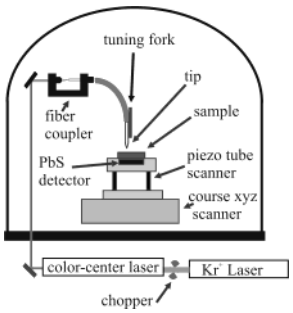

Figure 1. Schematic drawing of experimental setup.

Some of the better methods used to study vapor uptake in polymer films are Fourier transform infrared spectroscopy[17,22−24] and gravimetric analysis.[18−21] However, these methods do not provide the spatial resolution that IR-NSOM can; 300 nm spatial resolution has been achieved with transmission IR-NSOM at 3 μm in the infrared.[9−11] This paper describes the results of an IR-NSOM implemented in a controlled environment chamber to measure vapor uptake and swelling in polymers on a small spatial scale.

The infrared microscope is a variant based on the IR-NSOM apparatus developed by Dragnea et al.[9−11] A schematic diagram of the setup is shown in Figure 1. The NSOM was built inside a bell-jar environmental chamber capable of obtaining pressures

* To whom correspondence should be addressed. E-mail: srl@cchem.berkeley.edu.

[†] Current address: Departments of Chemistry and Physics, and Lawrence Berkeley National Laboratory, University of California, Berkeley, CA 94720.

[‡] Current address: Department of Chemistry, Indiana University, Bloomington, IN 47405-7102.

10.1021/jp022489j CCC: $25.00
Published on Web 05/02/2003

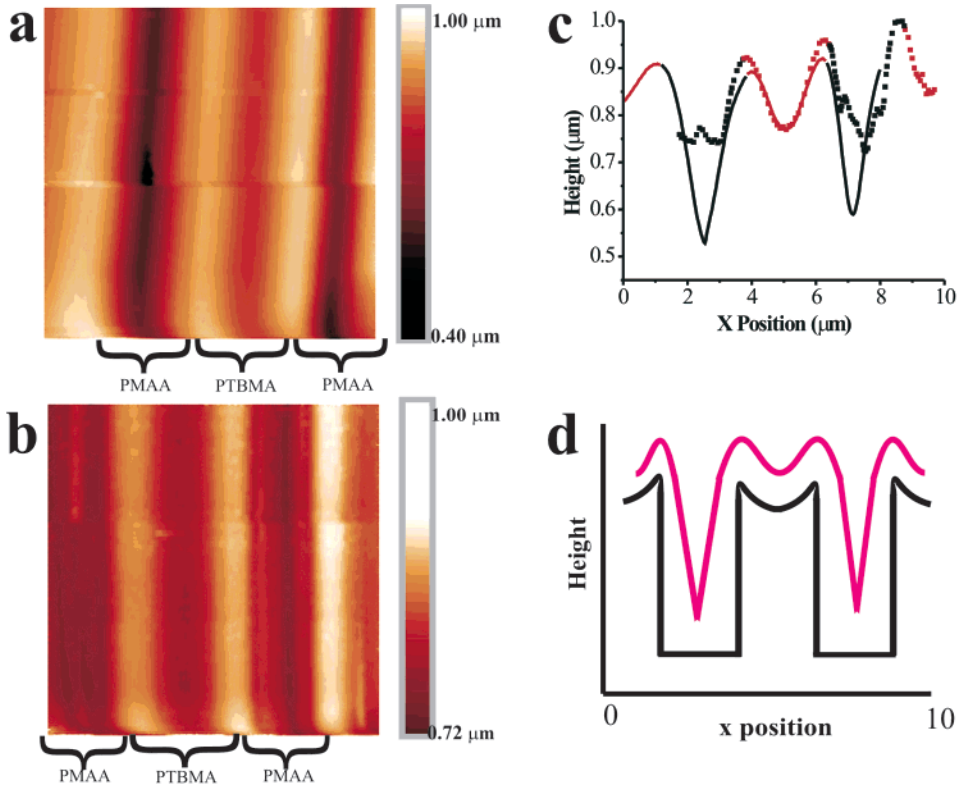

Figure 2. Topographic images of photolithographic polymers with 2 μm wide lines. Each image represents a single line scanned 256 times. (a) Topographic linescan of sample in a vacuum. (b) Topographic linescan of sample in 2.1 kPa water vapor environment. (c) Average line profiles. The solid line is an average profile of Figure 2a, and the dashed line is an average profile of Figure 2b. The red line portions represent PTBMA and the black lines represent PMAA. (d) A schematic drawing of the tip following the sample surface. The black line is a profile of the sample's topography, and the red line shows how the tip follows that surface to produce the topography image.

down to 13 Pa (0.10 Torr). A Kr^+ laser pumps a color-center laser, giving 2.6−3.2 μm infrared light, which is absorbed by the O−H stretching vibration of water vapor. For experiments described here, the laser was tuned to a wavelength of 2.85 μm.

The beam of infrared light enters the bell jar through a CaF_2 window in the chamber's base plate. The light is coupled into an infrared fiber composed of zirconium aluminum fluoride, which is transparent from 0.45 to 5.0 μm. The fiber is pulled into a tip at one end using a variable-pulling method.[9,10] The tip is coated with aluminum, typically leaving a 200 nm aperture. Because of the brittleness of the material, some of the tips used in this work may have fractured to sizes larger than 200 nm. The tip is suspended above the sample, which sits on an $x-y$ scanning stage moved by three piezoceramic tube legs. Directly below the sample is a large area, room temperature, PbS detector, which measures the transmission of the infrared light. The fiber tip is glued to a small tuning fork, which allows the topography to be measured via the shear-force feedback method.[25] The scanning and data acquisition are controlled by a scanning probe microscope controller.

All of the necessary alignment procedures are carried out before the chamber is evacuated. The IR beam is coupled into the fiber, and the tip is positioned above the sample in the near-field. Once the alignment is established, the glass bell jar is placed on the base plate and the chamber is pumped down. A picomotor screw allows for external control of the tip−sample distance in the z direction when the NSOM is enclosed. Up to 18 Torr of water vapor can be introduced to the chamber and is allowed to equilibrate for at least 45 min before a scan begins. In future work, real time measurements of uptake may be possible. Evident problems are the need to follow the changes in distances due to the polymer swelling and to adjust for changes in shear force feedback signals due to the water vapor environment.

Samples used are patterned, acid catalyzed, photolithographic polymers similar to those studied by Dragnea et al.[9−11] A 1.0 μm thick poly(*tert*-butylmethacrylate) (PTBMA) film containing the photoacid generator triphenylsulfonium hexafluoroantimonate was covered by a quartz/chrome mask and exposed to UV light in the range of 200−300 nm. The film was then baked at 130 °C for 5 min to activate the acid-catalyzed thermal deprotection chemistry. In the postexposure bake, the ester groups are converted to a hydrogen bonded carboxylic acid, poly(methacrylic acid) (PMAA), and the volatile product isobutylene is produced, thus shrinking the film substantially in the UV exposed regions. The modified polymer, PMAA, also has an OH stretching vibrational band, but by probing the sample with a wavelength (2.85 μm) that is strongly absorbed by the O−H stretch in water, the infrared light is only weakly absorbed by the PMAA's O−H bond. The resulting pattern used here has alternating 2 μm wide lines of approximately 1 μm thick PTBMA and 0.5 μm thick PMAA.

Images shown here are produced by scanning a line 256 times in the x direction, while disabling the scanning in the y direction. Each line scan also consists of 256 points. The transmission of light through the sample and the height of the tip above the sample are simultaneously recorded. The lines can be averaged and plotted to obtain a profile of the topography and transmission of the sample. This work shows two sets of measurements that compare the topography and optical properties of the sample in a vacuum conditions and in a water vapor environment.

Topographic images of the sample are shown in Figure 2. Figure 2a was recorded in a vacuum of 14 Pa pressure, whereas Figure 2b was measured in 2.1 kPa water vapor. Their average

line profiles are plotted together in Figure 2c to show that when exposed to a water vapor environment the gap between the highest point in the topography image and the lowest point is diminished. Figure 2c shows that the depth of the topographical valley is 0.4 μm in a vacuum; however, it is actually deeper because the tip cannot reach the bottom of the valley, because the tip is too wide. We know from atomic force microscopy (AFM) experiments done on the sample that the valley is actually 0.5 μm deep. Note also that the region containing PTBMA, the thicker polymer, is not flat. This structure is discussed in detail in previous work[11] and may be due to some combination of UV irradiation, edge enhancement and shrinkage. A schematic diagram of how the tip might follow the sample's topography is shown in Figure 2d.

Figure 2c shows that the depth of the valley for the sample under water vapor is only 220 nm. This indicates that the PMAA swells 280 nm more than PTBMA when exposed to 2.1 kPa water vapor. It is possible that the PTBMA also swells slightly, but we can only measure the relative change. The measured swelling suggests that the PMAA has absorbed more water than the PTBMA.

Figure 3, parts a and b, show the infrared transmission images recorded simultaneously with the topography images in Figure 2, parts a and b, respectively. Figure 3a, recorded under vacuum conditions, shows an image that is almost completely featureless, whereas Figure 3b shows large oscillations in the intensity of light reaching the detector. The reason is that one polymer absorbs more water than the other, thus allowing through less light. Again, the lines were averaged, and profiles of these images are plotted in Figure 3c. This graph shows a 6 $\pm$ 1% difference between the greatest and the smallest detected intensities. This number was obtained by taking the average of the two local maxima, subtracting the average of the two local minima, and then computing error bars using their standard deviations. It is obvious that this contrast is not due to a topographic artifact, because the transmission contrast increases while the topographic contrast decreases. However, the difference is not pure absorption contrast. There are several other contributing factors, which are discussed below.

The modified and unmodified polymers have different indices of refraction. This effect is explained by Dragnea et al.[9] as a change in cone angle of detection for our particular setup, and it is expected to produce a variation of 0.5%. It is this effect that causes a slight oscillation of the transmission signal in the vacuum case. Another contrast mechanism can be the change in index of refraction with concentration of water. During vapor uptake, a polymer's index will first increase as void-spaces are filled, and then the index can decrease as the film swells.[26] The changes in index of refraction will cause a further change in the amount of light transmitted to the PbS detector. Depending on the concentration of water in the film, this process can either enhance or diminish the transmission contrast. The OH stretching band of water can also change shape and shift in wavelength, depending on the concentration of water. Several examples are cited in the literature.[22−24] Although no specific studies have been done on PTBMA or PMAA, results on similar polymers indicate possible variations of approximately 0−5%. In addition, the absorption of light by the gas phase water vapor in the controlled environment chamber will create a baseline that must be subtracted. Another factor that could decrease the transmission contrast is the size of the NSOM aperture tip. When the tip's aperture is broken or too large, the transmission contrast is not as sharp or as great as it should be. All of these factors combined make it difficult to determine the concentration of

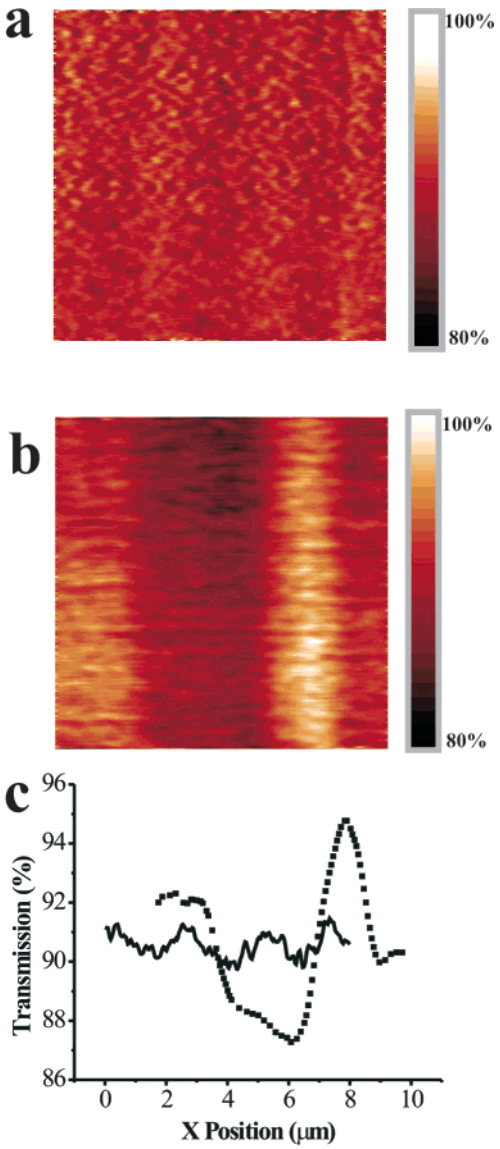

Figure 3. Transmission images of 2.85 μm light through photolithographic polymers with 2 μm wide lines. Each image represents a single line scanned 256 times. (a) Transmission linescan recorded in vacuum conditions. Darker regions represent smaller transmission intensity. (b) Transmission linescan recorded in 2.1 kPa water vapor environment. (c) Average line profiles of Figure 3, parts a and b. The solid line represents the average of Figure 3a, and the dashed line represents the average of Figure 3b.

water in the film. In the future, experiments with a quartz crystal microbalance will be performed simultaneously to quantitatively correlate the water concentration in the NSOM signals by more traditional gravimetric methods. Also, use of a tunable laser source to investigate band shifts will give access to information on water molecule interactions.

Optical and topographic images should be spatially consistent. The area that transmits less light should correspond to the region that swells more. However, in these particular images the optical images are shifted by 2 microns from the topographic images. This is known to be an artifact in these experiments because similar experiments on samples with 4 micron thick lines were also shifted by 2 microns. We do not know why the optical images were shifted, but we hypothesize that it may be image displacement due to the relatively large probe used. The point on the tip that is interacting with the sample to form the shear force image may be different from the optically transparent

region for the transmission intensity. Future work will correlate the transmission zones with the topographic images more rigorously.

To increase the quality of the images and the information obtained from the IR-NSOM described here, several changes to the experimental setup are required. First, detection should be improved by replacing the large area, room-temperature PbS detector with a liquid nitrogen cooled, small area, photovoltaic InSb detector.[10] Use of varying numerical aperture collection optics would help determine the contrast due to the cone angle effect.[9] Efforts can also be made to facilitate real-time measurements of vapor uptake. One way to achieve this would be to operate in constant height mode, rather than constant gap mode, so that the probe would not interact with the sample. To further improve the real-time measurements, we must determine the source of the variations in the shear-force feedback signals with change in water vapor pressure. Perhaps the use of a nonabsorptive glue to hold the fiber on the tuning fork will help solve stability problems.

This work demonstrates a new method for exploring the vapor uptake of polymers. The shear-force topographic method produces a value for the swelling of a polymer in a vapor environment and, with calibration of a known system, can become a precise measure of the amount of water absorbed in the sample. The transmission data complements the topographic images, and the results can be used to quantify the amount of water in a sample if more work is completed to separate the various contributing effects. Infrared NSOM under environmental control is an excellent potential new tool for determining where water vapor uptake occurs in a polymer sample on a small spatial scale.

Acknowledgment. We thank the National Science Foundation and the National Institute of Standards and Technology (NIST) for financial support of this project. Some of the equipment used for this research is on loan from NIST.

References and Notes

(1) Dragnea, B.; Leone, S. R. *Int. Rev. Phys. Chem.* **2001**, *20*, 59.
(2) Schaller, R. D.; Saykally, R. J. *Langmuir* **2001**, *17*, 2055.
(3) Stranick, S. J.; Chase, B.; Michaels, C. A. *Abstr. ACS* **2001**, *221*, 173.
(4) Cricenti, A. *J. Alloys Compd.* **2001**, *328*, 2.
(5) Hong, M. K.; Jeung, A. G.; Dokholyan, N. V.; Smith, T. I.; Schwettman, H. A.; Huie, P.; Erramilli, S. *Nucl. Instrum. Methods Phys. Res.* **1998**, *144*, 246.
(6) Knoll, B.; Keilmann, F. *Appl. Phys. A* **1998**, *66*, 477.
(7) Sahlin, J. J.; Peppas, N. A. *J. Appl. Polym. Sci.* **1997**, *63*, 103.
(8) La Rosa, A. H.; Yakobson, B. I.; Hallen, H. D. *Appl. Phys. Lett.* **1997**, *70*, 1656.
(9) Dragnea, B.; Preusser, J.; Schade, W.; Leone, S. R.; Hinsberg, W. D. *J. Appl. Phys.* **1999**, *86*, 2795.
(10) Dragnea, B.; Preusser, J.; Szarko, J. M.; Leone, S. R.; Hinsberg, W. *J. Vac. Sci. Technol. B* **2001**, *19*, 142.
(11) Dragnea, B.; Preusser, J.; Szarko, J. M.; McDonough, L. A.; Leone, S. R.; Hinsberg, W. *Appl. Surf. Sci.* **2001**, *175*−*176*, 783.
(12) Gray, M. H.; Hsu, J. W. P. *Rev. Sci. Instrum.* **1999**, *70*, 3355.
(13) Gray, M. H.; Hsu, J. W. P. *Appl. Phys. Lett.* **2000**, *76*, 1294.
(14) Elbs, H.; Fukunaga, K.; Stadler, R.; Sauer, G.; Magerle, R.; Krausch, G. *Macromolecules* **1999**, *32*, 1204.
(15) Padmanaban, M.; Endo, H.; Inoguchi, Y.; Kinoshita, Y.; Kudo, T.; Masuda, S.; Nakajima, Y.; Pawlowski, G. *Proc. SPIE* **1992**, *1672*, 141.
(16) MacDonald, S. A.; Cleacak, N. J.; Wendt, H. R.; Willson, C. G.; Snyder, C. D.; Knors, C. J.; Deyoe, N. B.; Maltabes, J. G.; Morrow, J. R.; McGuire, A. E.; Holmes, S. J. *Proc. SPIE* **1991**, *1466*, 2.
(17) Sutandar, P.; Ahn, D. J.; Franses, E. I. *Macromolecules* **1994**, *27*, 7316.
(18) Buchold, R.; Nakladal, A.; Gerlach, G.; Herold, M.; Gauglitz, G.; Sahre, K.; Eichhorn, K. J. *Thin Solid Films* **1999**, *350*, 178.
(19) Chen, W. L.; Shull, K. R.; Papatheodorou, T.; Styrkas, D. A.; Keddi, J. L. *Macromolecules* **1999**, *32*, 136.
(20) Hutcheon, G. A.; Messiou, C.; Wyre, R. M.; Davies, M. C.; Downes, S. *Biomaterials* **2001**, *22*, 667.
(21) Neogi, P. *Diffusion in Polymers*; Marcel Dekker: New York, 1996.
(22) Ping, Z. H.; Nguyen, Q. T.; Chen, S. M.; Zhou, J. Q.; D., D. Y. *Polymer* **2001**, *42*, 8461.
(23) Yarwood, J.; Sammon, C.; Mura, C.; Pereira, M. *J. Mol. Liq.* **1999**, *80*, 93.
(24) Linossier, I.; Gaillard, F.; Romand, M.; Feller, J. F.; Sci., J. A. P. *J. Appl. Polym. Sci.* **1997**, *66*, 2465.
(25) Karrai, K.; Grober, R. D. *Appl. Phys. Lett.* **1995**, *66*, 1842.
(26) Cross, G. H.; Ren, Y.; Swann, M. J. *Analyst* **2000**, *125*, 2173.